

Using S-Curve Transforms and Gamma Correction for MR Images Contrast Enhancement

*Manar A. Al-Abaji

Department of Computer Science, College of
Education for Pure Science, University of Mosul,
Nineveh, Iraq
[*manar_alabaji@uomosul.edu.iq](mailto:manar_alabaji@uomosul.edu.iq)

Zohair Al-Ameen

ICT Research Unit, Computer Center, University
of Mosul Presidency, University of Mosul,
Nineveh, Iraq
qizohair@uomosul.edu.iq

Abstract – Facilitating diagnosis and therapy. A common degradation in MR images is deficient contrast. This degradation affects the image with a layer of murkiness, reducing the clarity of details. Various contrast enhancement (CE) methods produce unsatisfactory results due to brightness amplification or artifact generation. Therefore, an effective CE algorithm called (WRGC) is introduced, which depends on two transformations of Weibull (W) and Rayleigh (R) distribution with modified gamma correction (GC), applied separately. The three resulting images are combined to obtain the features of all three images using an adapted logarithmic addition method. Finally, the output image is acquired by applying the normalization method. The proposed algorithm is tested with many degraded MR images obtained from the CTisus website. Moreover, it was compared with four different CE approaches and evaluated using three measures. The results showed that the proposed method outperformed many existing CE algorithms and provided satisfactory visual details and contrast-adjusted results.

Keywords: *S-curve Transform, Gamma correction, Contrast Enhancement, LIP, MRI.*



[Creative Commons Attribution-NonCommercial-ShareAlike 4.0 International License.](https://creativecommons.org/licenses/by-nc-sa/4.0/)

I. INTRODUCTION

Medical imaging technologies, including MRI, endoscope, X-ray, ultrasound, etc., utilize various approaches to see anatomical structures to diagnose dissimilar medical conditions. These technologies provide essential insights into multiple tissues and organs of the human body [1]. MRI images offer extensive medical information by capturing different images of numerous body regions without necessitating a change in body posture. It is a safe imaging modality that does not utilize radiation. Nonetheless, MR images are acquired with artifacts [2]. Since the human visual system gives 75% of the needed information [3], clear medical images help doctors diagnose and access important medical information [4].

CE is an essential step in medical image processing, as it plays a vital role in increasing the accuracy and usability of images in applications such as segmentation, analysis, and recognition. Good

contrast helps distinguish different tissues for segmentation, which facilitates dividing the image into regions with similar properties. While it enhances the ability of machine learning models to recognize patterns and features in images, such as tumors or pathological changes [5]. All of this helps to make more accurate and effective decisions, in addition to helping in early diagnosis of the disease, which contributes to saving thousands of patients [6].

CE seeks to increase the difference between the minimum and maximum image pixel values to better reveal its visual information. Low contrast indicates a minimal difference, whereas high contrast signifies a substantial difference. CE has been employed in several image processing applications as it directly alters the pixel distribution for a specified dynamic range [7]. Low contrast is a crucial problem in MR images since it obscures clarity and hinders the visibility of essential features. Furthermore, several concepts exist for CE, ranging from complex to simple, yet many have not achieved the anticipated improvement. An effective CE approach enhances the clarity of image information and details, which is essential for acquiring precise data for improved diagnosis [7]. This study presents an effective technique for improving the contrast of MR images.

Hence, a fast CE algorithm named WRGC is proposed to enhance the contrast of MR images. The WRGC utilizes a logarithmic image processing (LIP) addition model and gamma correction with two forms of S-curve transforms to modify the gray level of pixels. Initially, two forms of S-curve transformation (Weibull and Rayleigh distribution) and the Gamma correction are applied separately to the low-contrast MRI image. Then, the three outputs generated from the previous step are combined to obtain a new image containing the features of the three images using LIP. After that, a normalization method is applied to get the final image. Accordingly, the proposed algorithm is compared with four CE methods and three measures were used to calculate the accuracy and runtimes of the comparison. Promising results have been attained, and they are demonstrated and analyzed in the upcoming parts of the article. The other research sections are arranged as follows: Section 2 reviews the previous

studies. Section 3 explains the proposed algorithm. Section 4 demonstrates and discusses the results. Section 5 presents a brief conclusion.

II. RELATED WORKS

This section reviews different previous studies on contrast enhancement. Daniel et al. developed an algorithm that utilizes the Retinex theory. This study posits that the observed image has two elements: illumination and reflection. Using this concept, the disparity between the image's pixels and the mean center-surround of that pixel is computed [8]. Mikael et al. proposed the successive mean quantization transform technique, which enhances contrast through the set theory. This technique uses nonlinear stretching to preserve the original histogram's structure and can identify and break down the image's informational features to generate the output image [9].

Additionally, Huang et al. introduced a technique for adaptive gamma correction with a weighting distribution. This approach derives the image's spatial information using histogram analysis. The weighting distribution is simultaneously employed to mitigate artifacts and provide smoothness. Finally, an adaptive gamma correction is utilized to boost contrast automatically [10]. Moreover, Hoseini and Shayesteh proposed a hybrid approach by integrating ant colony optimization (ACO) with simulated annealing (SA) and a genetic algorithm (GA). SA with ACO facilitates the CE transform, while GA assists in adjusting the ACO parameters [11].

Furthermore, Chaira devised a CE method that employs fuzzy set theory. It generates a novel membership function utilizing the Hamacher T-Conorm, incorporating the lower and upper bound functions to adjust the contrast [12]. In addition, Kallel and Hamida proposed a technique based on the discrete wavelet transform (DWT) and singular value decomposition (SVD). DWT decomposes the image into four sub-bands. SVD is utilized on the LL sub-band to produce an improved LL. Based on the statistical data of the enhanced LL, it is processed by an adaptive gamma correction [13].

Additionally, Qingrong et al. proposed a technique that employs fuzzy theory. The image is broken down via the shearlet transform to extract its high and low parts. A thresholding technique then reduces the noise from the high component. A linear stretch method is utilized to improve the low component. Subsequently, the inverse transformation is executed on all components to recreate the image. Finally, a fast fuzzy CE method generates the final image [14]. Furthermore, Acharya and Ghoshal introduced an innovative technique utilizing skewness and mode-based histogram equalization. The image's histogram is first narrowed using a threshold derived from the skewness and subsequently partitioned into two segments depending on the mode value of the image. Each component is equalized and subsequently merged to produce the resulting image [15].

Rui et al. introduced a technique utilizing visual attention and image fusion. An attenuation weight matrix was used to adjust the contrast across several dimensions, and a specialized fusion technique generated the output image [16]. Moreover, Mnassri et al. introduced an innovative technique that relies on brightness-preserving dynamic fuzzy histogram equalization, singular value decomposition, and discrete wavelet transform. The process starts with image equalization via BPDFHE. Subsequently, the SVD is computed for the LL sub-bands of equalized and original images after DWT decomposes them to get the correction factor. After that, these LL sub-bands are reconstituted with the (HH, HL, LH) components of the original image. Finally, the IDWT is employed to obtain the final image [17].

Furthermore, Priyanshu et al. proposed an effective technique utilizing entropy curves and homomorphic filtering. This approach calculates the entropy value for each grey level to generate the image's entropy curve for enhancement purposes. Subsequently, homomorphic filtering diminishes noise and yields the resultant image [18]. Some previous studies on CE required a long processing time or adjustment of parameters. Furthermore, the others caused brightness augmentation or unwanted artifacts. Therefore, an efficient algorithm to enhance the contrast is needed, providing satisfactory performance and low complexity.

III. METHOD

This work presented an effective contrast enhancement algorithm for MR images. The proposed algorithm used S-curve transformations and the Gamma correction function to alter the gray level of the MR image. Then, LIP combined the resultant outputs and produced one image. After that, a normalization method is used to get an enhanced image. For in-depth details, the degraded MR image is initially processed by Weibull distribution (WD), Rayleigh distribution (RD), and gamma correction (GC). These approaches are applied separately to the input image to produce three modified gray-level images. Consequently, Eq. (1) illustrates the Weibull distribution function as follows [19]:

$$WD = 1 - \exp\left(-\left(\frac{x}{\alpha}\right)^r\right) \quad (1)$$

where (x) is the low-contrast MR image, (α) is a scaling parameter with $(\alpha > 0)$, (r) is the shape parameter, set to $(r = 0.9)$, and (WD) is the output of Weibull distribution. Furthermore, Eq. (2) represents the cumulative histogram of the Rayleigh distribution function, expressed mathematically as follows [20]:

$$RD = 1 - \exp\left(-\frac{x^2}{2\sigma^2}\right) \quad (2)$$

where (σ) is a scaling parameter, set to $(\sigma = 0.8)$, and (RD) is the resulting image. Next, the gamma

correction function is given by the following equation [21]:

$$GC = cx^\gamma \quad (3)$$

where (c) is a positive constant, (\cdot) is a multiplication operator, (γ) is the gamma factor, where using a higher value leads to more contrast representation, and (GC) is the processed image. Employing (γ) lower than 1 in a Gamma correction enhances a dark image, whereas utilizing (γ) higher than 1 enhances a bright image. In this work, (γ) is set to (1.5), and (c) is replaced by the exponential to reduce the parameters needed to adjust and better transform the image gray level depending on the image pixel values. The utilized gamma correction function becomes as follows:

$$GC = \exp(x) \cdot x^\gamma \quad (4)$$

At this stage, three altered gray-level images are acquired. One method to include the features of several images in a new one is by the application of LIP addition mode, one particular model of interest being the following [22]:

$$u \oplus v = 1 - \frac{(1-u) \cdot (1-v)}{1-u \cdot v} \quad (5)$$

where (u and v) are two images, and (\oplus) is the addition operator in LIP. This model combined the features of two images, (u) and (v), to produce one new image containing their features. This work used a modified version of this model to get the features of the three images resulting from the WD, RD and GC to produce a new image (F). The modified version of the model is as follows:

$$F = 1 - \frac{(1-WD) \cdot (1-RD) \cdot (1-GC)}{1-(WD \cdot RD)} \quad (6)$$

where WD, RD, and GC are three images resulting from applying Weibull distribution, Rayleigh distribution, and Gamma correction, respectively, and (F) is the resulting image from the LIP process. To complete the developed algorithm, image (F) is normalized to the whole range utilizing the following equation [23]:

$$M = \frac{F - F_{\min}}{F_{\max} - F_{\min}} \quad (7)$$

where (F_{\min}) and (F_{\max}) are the lowest and highest values in F, and (M) is the final enhanced MR image. For better comprehension, the algorithm's flowchart is presented in Figure 1.

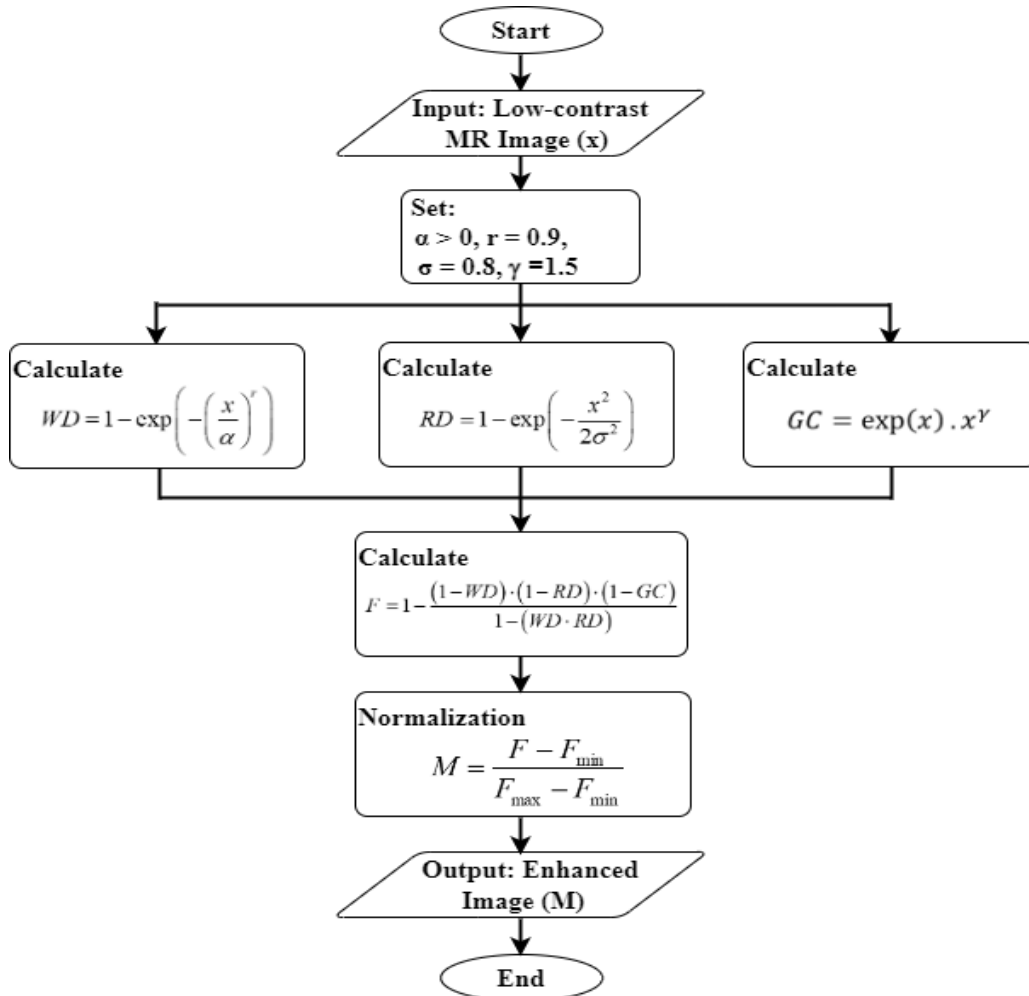


Figure 1. The Proposed Algorithm

IV. RESULTS AND DISCUSSION

This section encompasses information on the dataset, testing processes, comparatives, quality assessment metrics, and computer specifications. The dataset was obtained from the CTisus medical repository, accessible at <https://www.ctisus.com/>. A collection of varied real low-contrast images was amassed from the given medical cases. The comparison involves four dissimilar algorithms that employ various processing concepts, as previously discussed in the related works section: SSR [8], Fuzzy [12], AGCWD [10], and SMQT [9]. The resultant images from the comparisons are assessed utilizing NSS [24], BRISQUE [25], and runtimes. Natural Scene Statistics (NSS) quantifies the naturalness of contrast. To evaluate quality, NSS identifies various characteristics, including moment and entropy. An NSS model is constructed for each feature. A fusion

approach is subsequently employed to integrate these models, yielding an effective metric for predicting the quality.

Blind Referenceless Image Spatial Quality Evaluator (BRISQUE) assesses images' overall quality. It presents a novel model grounded in locally normalized brightness statistical measurements. These measures demonstrate quantitative outcomes, wherein a greater NSS with lower BRISQUE signifies superior quality. All developments, tests, and comparisons were executed via a laptop equipped with a CPU of an Intel Core i7-10510U and RAM of 16 GB. Figures (2) and (3) present some results of the tests, whereas Figures (4) through (7) illustrate the comparative results. Table (1) presents the objective assessment scores of the comparison and the implementation time. Figures (8) through (10) show the evaluation scores as charts.

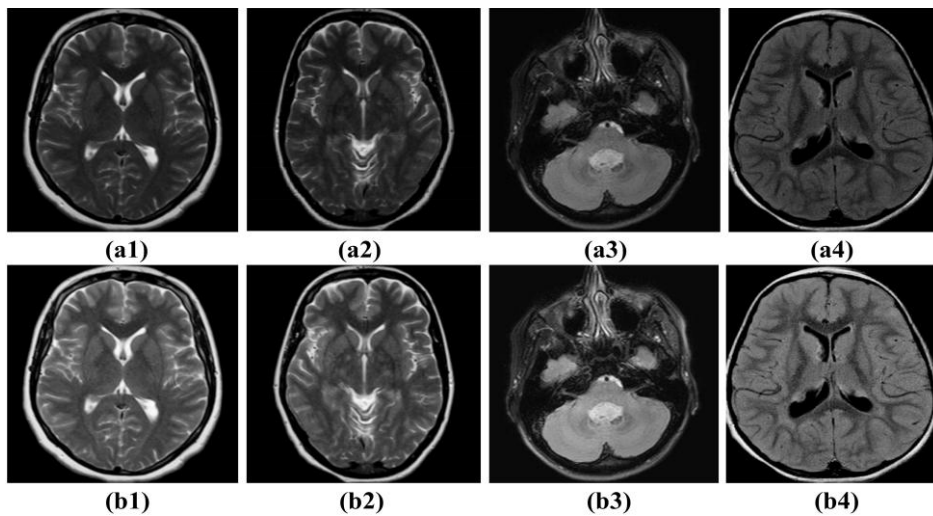


Figure 2. Images resulted from applying the WRGC algorithm (Set 1). (a1-a4) low contrast MR images; (b1-b4) processed MRI images with $\alpha = (0.5, 0.55, 0.7, 0.52)$.

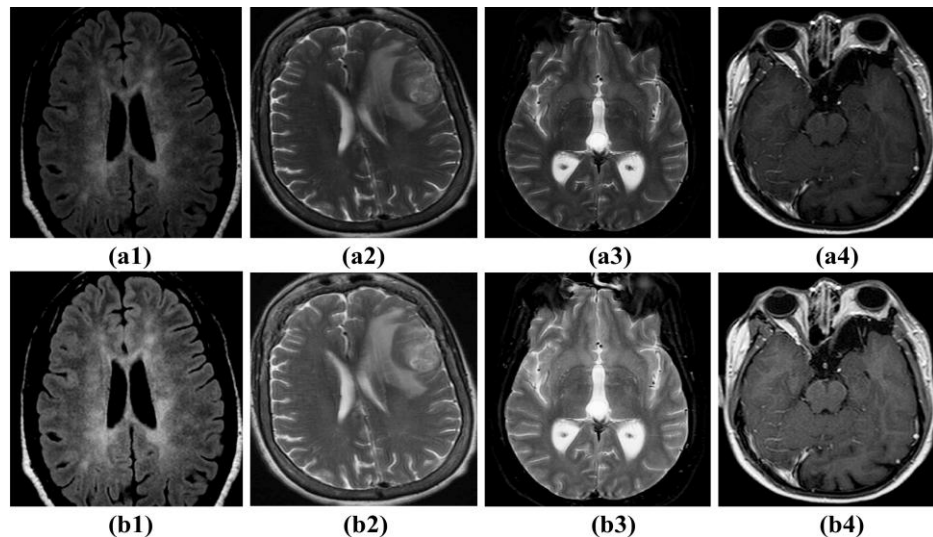


Figure 3. Images resulted from applying the WRGC algorithm (Set 2). (a1-a4) low contrast MR images; (b1-b4) processed MRI images with $\alpha = (0.6, 0.55, 0.48, 0.51)$.

The results in Figures 2 and 3 illustrate the algorithm's capabilities in processing various degraded MR images. The proposed algorithm yields outcomes with satisfactory appearance and adequate

contrast while preventing excessive amplification of bright regions and enhancing the clarity of details in darker areas without noticing artifacts. This success applies to diverse images exhibiting different contrast

distortions. Moreover, the comparison with other methods gave dissimilar performances acquired, and the ability of each method across each measure is graded from lower to higher as follows: lower, low, medium, high, and higher. The runtimes of the algorithms were assessed based on the results acquired, and all analyses depended on the average performance metrics for each measurement.

MR images with low contrast exhibit a fog-like appearance, attributable to the imaged tissue's characteristics, which may possess identical signal intensity levels, while others are related to the selection of imaging equipment settings or the application of inefficient image processing methods. Applying the SSR algorithm on degraded images resulted in unnatural contrast, causing the darkening of several regions, which rendered the final image unnatural. This accounts for its higher BRISQUE score and lower NSS value. This method was placed fourth in terms of processing time.

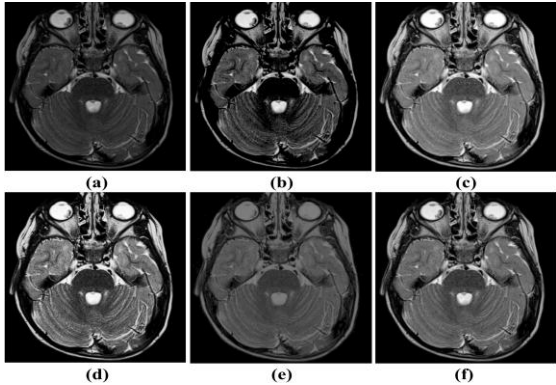


Figure 4. Images resulted from the comparisons (Set 1). (a) Low contrast Image; (b) SSR; (c) FuzzyII; (d) AGCWD; (e) SMQT; (f) Proposed WRGC with $\alpha = (0.6)$.

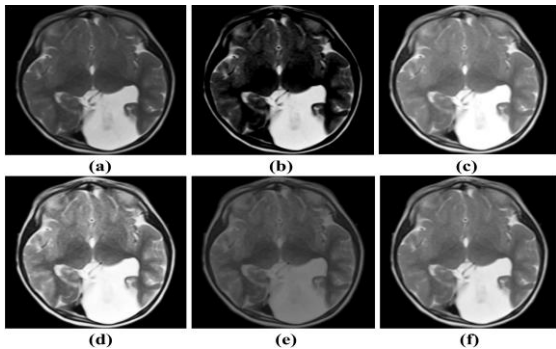


Figure 5. Images resulted from the comparisons (Set 2). (a) Low contrast Image; (b) SSR; (c) FuzzyII; (d) AGCWD; (e) SMQT; (f) Proposed WRGC with $\alpha = (0.6)$.

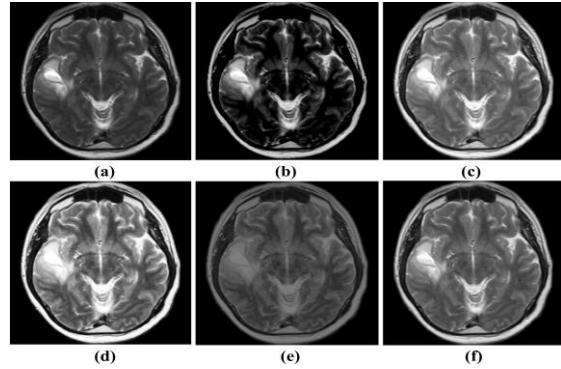


Figure 6. Images resulted from the comparisons (Set 3). (a) Low contrast Image; (b) SSR; (c) FuzzyII; (d) AGCWD; (e) SMQT; (f) Proposed WRGC with $\alpha = (0.6)$

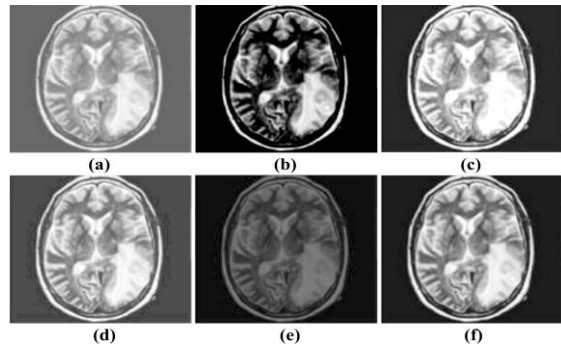


Figure 7. Images resulted from the comparisons (Set 4). (a) Low contrast Image; (b) SSR; (c) FuzzyII; (d) AGCWD; (e) SMQT; (f) Proposed WRGC with $\alpha = (0.6)$.

The FuzzyII algorithm demonstrated good performance. Despite its tendency to increase brightness slightly, it produces images with clear detail visibility and natural contrast. This explains its high value in NSS and low value in BRISQUE. It also documented a superior processing speed relative to other algorithms. The AGCWD algorithm generated images with adequate clarity; nevertheless, it heightened brightness, resulting in a rather restricted intensity distribution across the image range. Consequently, it exhibited a low value in NSS and an average value in BRISQUE. It ranked second in processing time among the utilized algorithms.

The SMQT algorithm produced images with consistent contrast; however, it unusually restricted brightness in the bright regions. This illustrates why it received an average score in NSS and a high score in BRISQUE. This indicates that these constraints were considered in the metrics. Regarding implementation duration, this method was slower than the other comparison algorithms. Although the proposed WRGC algorithm yielded a moderate processing time, it generated clear images with naturalistic contrast and effectively lit dark areas without undesired amplification. Therefore, it achieved the best performance based on BRISQUE and NSS metrics. This is highly important in processing MR images since a non-complex algorithm has been established that produces results with satisfactory visibility.

Table 1. The quality metrics scores and the run time of the comparison.

Methods	Fig	BRISQUE ↓	NSS ↑	Run Time
SSR	4	51.425	2.155	0.314
	5	51.799	2.095	0.037
	6	53.574	2.113	0.033
	7	54.563	2.256	0.020
	Average	52.840	2.155	0.101
FuzzyII	4	51.524	2.387	0.118
	5	49.283	2.297	0.024
	6	50.486	2.396	0.022
	7	52.863	2.430	0.010
	Average	51.039	2.378	0.044
AGCWD	4	53.717	2.132	0.179
	5	49.925	2.405	0.031
	6	51.824	2.027	0.032
	7	50.546	2.324	0.049
	Average	51.503	2.222	0.073
SMQT	4	50.921	2.320	1.765
	5	50.916	2.408	0.385
	6	51.825	2.318	0.352
	7	55.940	2.103	0.088
	Average	52.400	2.287	0.647
Proposed WRGC	4	50.237	2.468	0.251
	5	48.359	2.491	0.025
	6	49.516	2.494	0.023
	7	50.516	2.519	0.017
	Average	49.657	2.493	0.079



Figure 8. Average BRISQUE Scores.

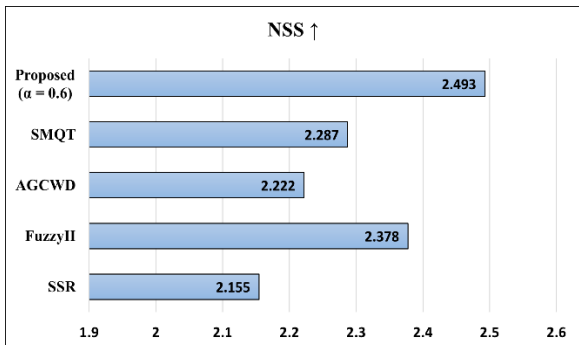


Figure 9. Average NSS Scores.

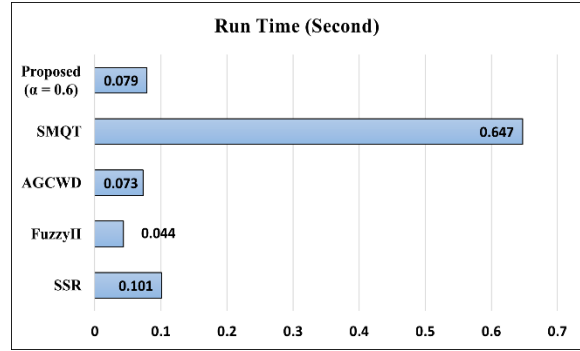


Figure 10. Average Execution Times.

V. CONCLUSION

This research developed a statistics-based algorithm to enhance the contrast of MR images. The presented algorithm comprises several uncomplicated, integrated, and tailored methods to execute a satisfactory CE model. Examining numerous real low-contrast MR images yielded acceptable results for brightness retention, contrast enhancement, and overall visual appeal. This algorithm has five procedures executed by low-complexity methods. In this context, the brightness of the darker regions has been enhanced while preventing excessive amplification in the brighter areas. The comparison demonstrated the superiority of the proposed algorithm over several others, excelling both subjectively and objectively while maintaining relatively modest implementation times. As a future work, a further enhancement of this algorithm can be employed using other less complexity statistical methods.

REFERENCES

- [1] S. Naidu, P. Parvatkar, A. Quadros, K. C. Kumar, A. Natekar, and S. Aswale, "Medical Image Enhancement based on Statistical and Image Processing Techniques," *Int. J. Eng. Res. Technol.*, vol. 10, no. 05, pp. 509–515, 2021.
- [2] U. Singh and M. K. Choubey, "A Review: Image Enhancement on MRI Images," 2021 5th Int. Conf. Inf. Syst. Comput. Networks, ISCON 2021, pp. 2–7, 2021, doi: 10.1109/ISCON52037.2021.9702464.
- [3] A. Taha and S. Ebraheem, "A survey on tamper detection techniques for digital images," *AL-Rafidain J. Comput. Sci. Math.*, vol. 16, no. 2, pp. 15–23, Dec. 2022, doi: 10.33899/csmj.2022.176585.
- [4] R. M. HASAN and I. O. A. MAJJED, "Comparison between different methods for identifying lesion in pulmonary x-ray images," *MINAR Int. J. Appl. Sci. Technol.*, vol. 03, no. 03, pp. 77–86, Sep. 2021, doi: 10.47832/2717-8234.3-3.10.
- [5] R. S. Mahamed Najeeb and I. O. Abdul Majjed, "Brain Tumor Segmentation Utilizing Generative Adversarial, Resnet And Unet Deep Learning," in 2022 8th International Conference on Contemporary Information Technology and Mathematics (ICCITM), IEEE, Aug. 2022, pp. 85–89. doi: 10.1109/ICCITM56309.2022.10031760.
- [6] M. M. Al-Anezi, M. J. Mohammed, and D. S. Hammadi, "Artificial immunity and features reduction for effective breast cancer diagnosis and prognosis," *Int. J. Comput. Sci. Issues*, vol. 10, no. 3, p. 136, 2013.

- [7] G. Cao, H. Tian, L. Yu, and X. Huang, "Fast contrast enhancement by adaptive pixel value stretching," *Int. J. Distrib. Sens. Networks*, vol. 14, no. 8, 2018, doi: 10.1177/1550147718793803.
- [8] D. J. Jobson, Z. U. Rahman, and G. A. Woodell, "Properties and performance of a center/surround retinex," *IEEE Trans. Image Process.*, vol. 6, no. 3, pp. 451–462, 1997, doi: 10.1109/83.557356.
- [9] M. Nilsson, M. Dahl, and I. Claesson, "The Successive Mean Quantization Transform," *ICASSP, IEEE Int. Conf. Acoust. Speech Signal Process. - Proc.*, vol. IV, no. 1, pp. 429–432, 2005, doi: 10.1109/ICASSP.2005.1416037.
- [10] S. C. Huang, F. C. Cheng, and Y. S. Chiu, "Efficient contrast enhancement using adaptive gamma correction with weighting distribution," *IEEE Trans. Image Process.*, vol. 22, no. 3, pp. 1032–1041, 2013, doi: 10.1109/TIP.2012.2226047.
- [11] P. Hoseini and M. G. Shayesteh, "Efficient contrast enhancement of images using hybrid ant colony optimisation, genetic algorithm, and simulated annealing," *Digit. Signal Process. A Rev. J.*, vol. 23, no. 3, pp. 879–893, 2013, doi: 10.1016/j.dsp.2012.12.011.
- [12] T. Chaira, "An improved medical image enhancement scheme using Type II fuzzy set," *Appl. Soft Comput.*, vol. 25, pp. 293–308, Dec. 2014, doi: 10.1016/j.asoc.2014.09.004.
- [13] F. Kallel and A. Ben Hamida, "A New Adaptive Gamma Correction Based Algorithm Using DWT-SVD for Non-Contrast CT Image Enhancement," *IEEE Trans. Nanobioscience*, vol. 16, no. 8, pp. 666–675, 2017, doi: 10.1109/TNB.2017.2771350.
- [14] G. Qingrong, J. Zhenhong, Y. Jie, and N. Kasabov, "Contrast enhancement of medical images using fuzzy set theory and nonsubsampling shearlet transform," *Int. J. Imaging Syst. Technol.*, vol. 29, no. 4, pp. 483–490, 2019, doi: 10.1002/ima.22326.
- [15] K. Acharya and D. Ghoshal, "Contrast Enhancement of Images through Skewness and Mode Based Bi-Histogram Equalization," *Int. J. Image, Graph. Signal Process.*, vol. 12, no. 5, pp. 13–27, 2020, doi: 10.5815/ijgisp.2020.05.02.
- [16] R. Zhu, X. Li, X. Zhang, and X. Xu, "MRI enhancement based on visual-attention by adaptive contrast adjustment and image fusion," *Multimed. Tools Appl.*, vol. 80, no. 9, pp. 12991–13017, Apr. 2021, doi: 10.1007/s11042-020-09543-9.
- [17] B. Mnassri, F. Kallel, A. Echioui, A. Ben Hamida, M. Dammak, and C. Mhiri, "MRI contrast enhancement using singular value decomposition and brightness preserving dynamic fuzzy histogram equalization applied to multiple sclerosis patients," *Signal, Image Video Process.*, vol. 17, no. 5, pp. 2035–2043, 2023, doi: 10.1007/s11760-022-02416-8.
- [18] P. S. Yadav, B. Gupta, and S. S. Lamba, "A new approach of contrast enhancement for Medical Images based on entropy curve," *Biomed. Signal Process. Control*, vol. 88, no. PB, p. 105625, 2024, doi: 10.1016/j.bspc.2023.105625.
- [19] C. A. Game, M. B. Thompson, and G. D. Finlayson, "Weibull Tone Mapping (WTM) for the Enhancement of Underwater Imagery," *Sensors*, vol. 23, no. 7, p. 3533, Mar. 2023, doi: 10.3390/s23073533.
- [20] H. Z. Muhammed and H. M. Abdelghany, "Modified Weighted Rayleigh Distribution and Its Bivariate Extension," *J. Probab. Stat. Sci.*, vol. 21, no. 1, pp. 60–83, Mar. 2023, doi: 10.37119/jpss2023.v21i1.640.
- [21] S. Rahman, M. M. Rahman, M. Abdullah-Al-Wadud, G. D. Al-Quaderi, and M. Shoyaib, "An adaptive gamma correction for image enhancement," *EURASIP J. Image Video Process.*, vol. 2016, no. 1, p. 35, Dec. 2016, doi: 10.1186/s13640-016-0138-1.
- [22] C. FLOREA and L. FLOREA, "Logarithmic Type Image Processing Framework for Enhancing Photographs Acquired in Extreme Lighting," *Adv. Electr. Comput. Eng.*, vol. 13, no. 2, pp. 97–104, 2013, doi: 10.4316/AECE.2013.02016.
- [23] Z. Al-Ameen, Z. Younis, and S. Al-Ameen, "HLIPSCS: A Rapid and Efficient Algorithm for Image Contrast Enhancement," *Int. J. Comput. Digit. Syst.*, vol. 12, no. 2, pp. 311–320, Jul. 2022, doi: 10.12785/ijcds/120125.
- [24] Y. Fang, K. Ma, Z. Wang, W. Lin, Z. Fang, and G. Zhai, "No-Reference Quality Assessment of Contrast-Distorted Images Based on Natural Scene Statistics," *IEEE Signal Process. Lett.*, vol. 5, no. 7, pp. 1–1, 2014, doi: 10.1109/LSP.2014.2372333.
- [25] T. Sun, X. Zhu, J.-S. Pan, J. Wen, and F. Meng, "No-Reference Image Quality Assessment in Spatial Domain," in *Genetic and Evolutionary Computing*, vol. 21, no. 12, 2015, pp. 381–388. doi: 10.1007/978-3-319-12286-1_39.